Romanian Reports in Physics, Vol. 68, No. 1, P. 416–424, 2016

REVISED PALEOSECULAR VARIATION FROM QUATERNARY LAVA FLOWS FROM THE EAST CARPATHIANS

C.G. PANAIOTU[1], D. DIMOFTE[1], C. NECULA[1], A. DUMITRU[1], I. SEGHEDI[2], R.-G. POPA[2]

[1] University of Bucharest, Paleomagnetic Laboratory, Faculty of Physics, Bucharest, Romania, E-mail: cristian.panaiotu@g.unibuc.ro
[2] Romanian Academy, Institute of Geodynamics, Bucharest, Romania

Received February 22, 2015

Abstract. This study presents new paleomagnetic results from 17 sites in the lava flows younger than 1.1 Ma from the East Carpathians. Based on these new data and previous results, we show that there is a significant change in the paleosecular variation of the geomagnetic field after 1 Ma at around 46°N.

Key words: paleomagnetism, paleosecular variation, Quaternary lavas, East Carpathians.

1. INTRODUCTION

The structure and evolution of the geomagnetic field is important to understanding the geodynamo and Earth's deep interior. Many aspects of its behavior are not well documented mainly on timescales of 10^4 to 10^6 years. Paleosecular variation of the geomagnetic field is increasingly viewed as one of the most important tools for studying changes at this time scale in the behavior of the geodynamo. During the past 15 years, multiple studies were conducted to obtain high quality palaeomagnetic records from lava flows that document the paleosecular variation in the last 5 Ma [1, 2].

The post-collisional lava flows from the East Carpathian has created the opportunity to study the paleosecular variation of the geomagnetic field in the last 11 Ma. The progressive migration of the volcanic activity from north to south allows to studying the time variation of the paleosecular variation in time slices of 1-2 Ma. The research is in progress and up to now we have study the lava flows erupted in the last 4 Ma in the South Harghita Mountains [3] and the Perşani Mountains [4]. Because these previous studies have provided only 26 sites younger than 1.1 Ma, we have sampled new sites to obtain a better estimation of the paleosecular variation in the last 1 Ma.

2. SAMPLING AREA AND METHODS

We have sampled 4 new sites in the Ciomadu volcanic structure and 13 new sites in the basalts from the Perşani Mountains (Fig. 1). The age of the sampled rocks is between 1.1 Ma and 0.6 Ma for the Perşani basalts [4] and between 0.7 Ma and 0.4 Ma for the Ciomadul dacites [5]. Each site consisted of 6–10 oriented samples. The samples were oriented using a Brunton magnetic compass and a sun compass where possible. The location of the new sampling sites is presented in Table 1.

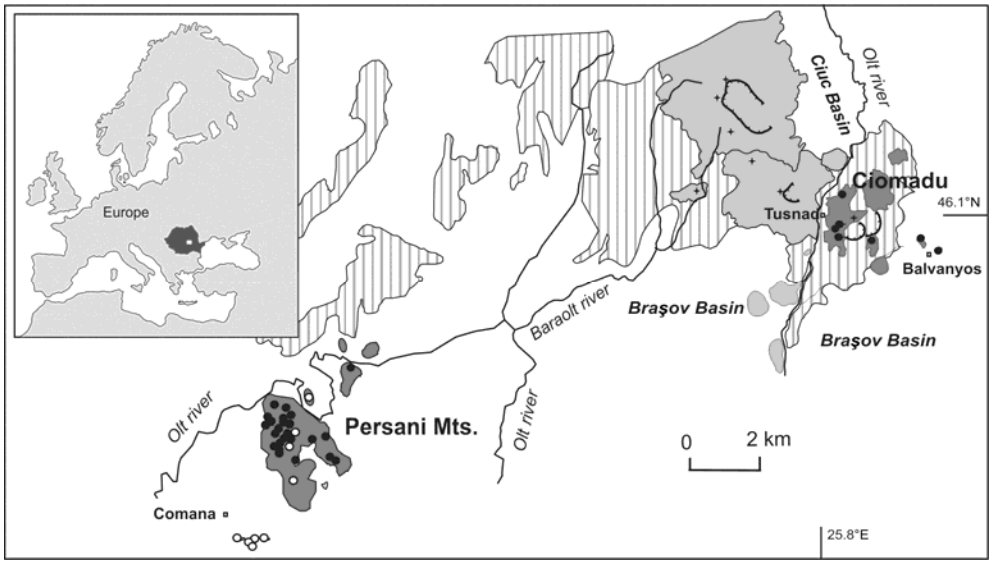

Fig. 1 – Sketch map of the sampling areas. Dark grey areas mark the sampling areas in the Quaternary volcanic regions from the Perşani Mountains and Ciomadul. Older volcanic rocks are marked with light grey. Volcanoclastic areas are marked with vertical grey lines. Paleomagnetic sites: full circles = normal polarity; empty circles = reversed polarity. The inset show the position of Romania in Europe and the white spot marks the position of the sketch map.

Laboratory analyses were carried out in the Palaeomagnetic Laboratory at the University of Bucharest. Standard paleomagnetic specimens (11 cm^3) were cut from each core. Remanent magnetizations were measured using a JR6A spinner magnetometer (AGICO). Alternating-field (AF) demagnetization was done using either a LDA-3A – AF demagnetizer (AGICO) or a static AF demagnetizer (Magnon International). AF demagnetization was performed in steps from 0 to maximum 100 mT, with 7 to 10 steps per specimen. For some specimens the AF demagnetization was followed by thermal demagnetization between 450°C and

650 °C to fully demagnetize the samples. Thermal demagnetization was performed with a Thermal demagnetizer TD 700 (Magnon International). The susceptibility variation upon thermal treatment was measured on MFK1-A kappabridge (AGICO). Demagnetization data were plotted on orthogonal demagnetization diagrams and magnetization components were isolated by principal component analysis using the Remasoft 3.0 software [6]. The line fits were based on the following constrains: 1. minimum 4 demagnetization steps; 2. the line fit was anchored to the origin; 3. the maximum angular deviation was less than 5°. Statistical analysis of directional data was done using Lisa Tauxe's PmagPy-2.171 software package [7].

Several rockmagnetic properties were measured for each site to determine the ferromagnetic mineralogy. The field dependence of the magnetic susceptibility between 2 A/m and 700 A/m was determined using the MFK1A kappabridge (AGICO). These curves were characterized using the V parameter [8]. This parameter is define as $V = 100(k_{700}–k_{50})/k_{50}$, where k_{50} and k_{700} are the susceptibilities measured at 50 and 700 A/m, respectively. A sample from each site was magnetized in a 2 T magnetic field using a pulse magnetizer MMPM10. The acquired isothermal remanent magnetization (IRM_{2T}) was measured using a JR5 spinner magnetometer. Then we applied a 0.3 T back field and the remaining remanent magnetization ($IRM_{0.3T}$) was measured. The S ratio was calculated as $–IRM_{03T}/IRM_{2T}$. S-ratio is used to estimate the relative content of ferrimagnets (such as magnetite) *versus* antiferrimagnets (such as hematite) [9].

3. RESULTS

3.1. ROCKMAGNETISM

The values of V parameter and S ratio are plotted in Fig. 2. The V parameter for basalt samples range from around 1% to 63% and the S ratio is above 0.97 with one exception. The analyzed basalts have a variable ferromagnetic mineralogy from magnetite with no field dependence to titanomagnetite with increasing Ti content and field dependence. These results are similar to those obtained in the previous studies from the Perşani basalts [4, 10]. The ferromagnetic minerals identified in the Ciomadul dacites are magnetite and hematite (S ratio between 0.82 and 0.69, V parameter around 0). The same mineralogy was also identified in other studies from this area [3, 11].

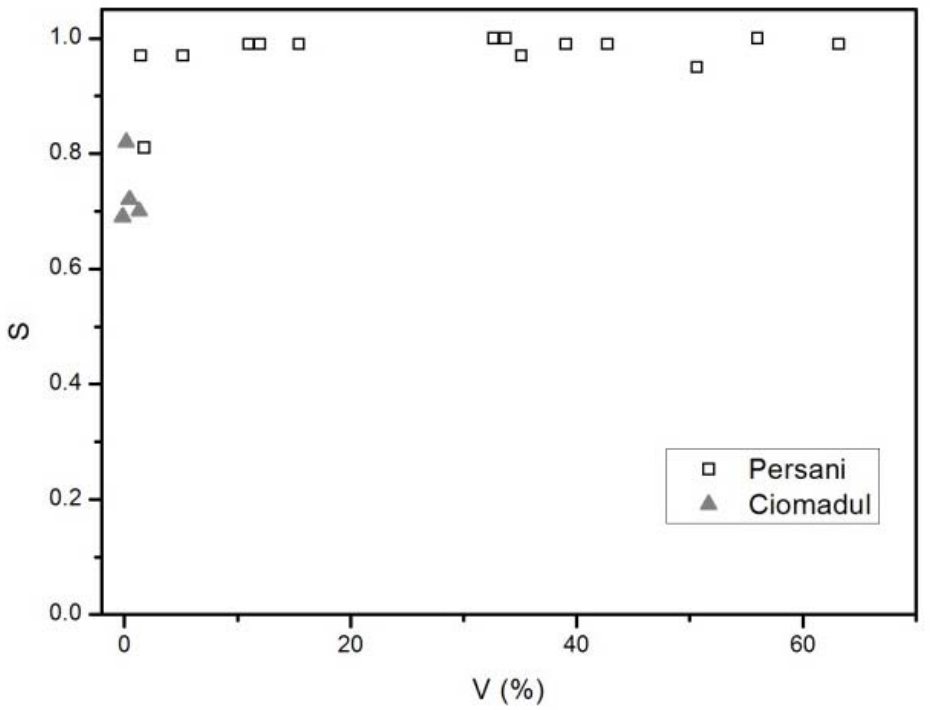

Fig. 2 – S ratio *versus* V parameter.

3.2. PALEOMAGNETIC RESULTS

Natural remanent magnetization and demagnetization behavior were measured on a total of 97 independent samples. Representative examples of demagnetization curves are presented in Fig. 3. Most of basalts specimens were AF demagnetized. The specimens with a mixt ferromagnetic mineralogy, magnetite and hematite, were first AF demagnetized and then thermal demagnetized between 450 °C and 650 °C. Primary characteristic component was unambiguously identified in all analyzed samples. In some samples soft components, considered viscous overprints, were observed, but they were usually removed at demagnetization steps below 20 mT. Site mean directions were calculated using Fisher statistics [12]. The new site mean directions and virtual geomagnetic poles (VGP) together with previous results from Perşani Mountains [4] and Ciomadul volcanic structure [3] are presented in Table 1.

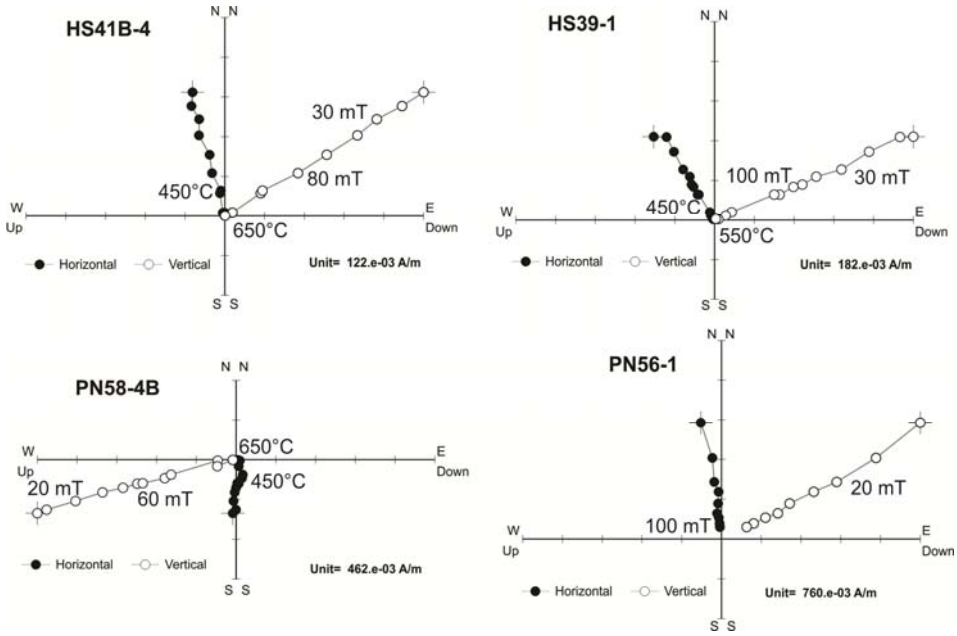

Fig. 3 – Typical examples of demagnetization diagrams.

Table 1

Declination (*D*), inclination (*I*), number of specimens (*N*), precision parameter (*k*), confidence angle (α_{95}), VGP latitude (Plat) and VGP longitude (Plong) for site mean directions. References (Ref) for the data according to [3, 4] and this study

Site	Site latitude (°N) /longitude (°E)	*D* (°)	*I* (°)	*N*	*k*	α_{95} (°)	Plong (°)	Plat (°)	Ref
Perşani basalts (age between 1.1–0.6 Ma [4])									
PN35	45.890317/25.302600	168.1	-69.0	5	254	4.8	144	-66.2	[4]
CO	45.892283/25.311933	152.5	-61.7	6	295	4.4	116.1	-70.2	[4]
PN51	45.881644/25.297281	144.1	-61.7	6	166	5.2	121.7	-64.4	This study
PN52	45.884234/25.296670	198.6	-60.7	6	401	3.3	305.8	-76	This study
PN53	45.894210/25.282985	184.8	-73.3	6	166	5.2	305.8	-76.6	This study
TZ	46.001796/25.354147	168.1	-57.1	6	140	4.3	76.2	-77.9	[4]
PN14	46.062100/25.409000	357.2	49.2	5	132	6.7	237.3	73	[4]
PN17	45.989433/25.339733	23.8	61	5	115	7.2	115.0	75.5	[4]
PN21	45.981683/25.351000	10.7	60.2	6	54	9.1	180.1	70.5	[4]
PN18	45.980167/25.311017	17.0	64.1	6	91	7.0	87.1	73.7	[4]
PN19	45.979417/25.311250	31.9	64.5	6	177	5	93.3	61.6	[4]
PN20	45.978850/25.312667	15.5	62.5	6	94	6.9	114.8	75.3	[4]

Table 1

(continued)

Site	Site latitude (°N) /longitude (°E)	*D* (°)	*I* (°)	*N*	*k*	α_{95} (°)	Plong (°)	Plat (°)	Ref
PN22	45.955717/25.352850	10.9	51.7	5	63	9.6	237.3	79.5	[4]
PN23	45.957719/25.353293	19.4	62.7	7	234	4	95.1	79.9	[4]
PN24	45.959667/25.352167	7.3	72.1	6	286	4	358.6	79.2	[4]
PN28	45.956183/25.352517	6.9	75.7	6	401	3.3	4.6	74.7	[4]
PN27	45.954950/25.351317	342.3	75	6	128	5.9	-1.0	71.1	[4]
PN45	45.963367/25.344033	335.2	64.2	5	153	6.2	302.5	72.2	[4]
PN33	45.966067/25.343733	36.2	63	5	310	4.3	115.1	68.2	[4]
PN32	45.968000/25.344567	15.6	77.6	7	153	4.9	39.9	55.5	[4]
PN47	45.968000/25.342167	340.9	61.3	6	201	4.7	333.1	69.7	[4]
BV1	45.971638/25.344882	20.7	57.2	5	76	8.8	136.1	72.6	[4]
PN36	45.945050/25.365533	341.1	69.8	8	173	4.2	22.1	76.4	[4]
PN34	46.018267/25.408950	346.4	64.5	6	571	2.8	298.1	78.3	[4]
BAQ	45.956467/25.354650	220.3	-54.0	6	320	3.7	301.5	-57.6	[4]
BQ	45.962781/25.351701	228.3	-50.9	12	283	5.5	305.3	-50.6	[4]
PN50	45.947298/25.381286	29.7	72.9	6	1128	2	69.7	68.2	This study
PV	45.943867/25.387200	11.1	72.5	12	2237	2.6	49.3	73.4	[4]
PN54	45.961894/25.377427	358.8	72.2	6	118	6.2	22.2	78.6	This study
PN55	45.956138/25.365931	359.7	72.3	6	294	3.9	24.6	78.6	This study
PN56	45.960924/25.333266	344.2	62	5	118	7.1	-47.4	81.9	This study
PN57	45.926240/25.344903	171.9	-71.0	10	179	3.6	-153.6	-72.6	This study
PN59	45.944977/25.341871	331.9	61.7	5	663	3	-55.6	72.1	This study
PN60	45.947432/25.342688	330.6	59.4	5	403	3.8	-88.1	68.3	This study
PN61	45.950451/25.342364	327.7	60.9	5	418	3.7	-52.9	66.1	This study
PN62	45.950626/25.344505	333.4	59.5	5	114	7.2	-62	68.9	This study
PN63	45.949146/25.343656	325.8	58.8	5	840	2.6	-61.7	66.1	This study
Ciomadul dacites (age between 1 – 0.4 Ma [5])									
HS22	46.150033/25.879617	0.1	69.5	8	230	3.7	26.4	83.0	[3]
HS39	46.135289/25.883574	320.8	69.3	5	121	7	-34.6	64.0	This study
HS40	46.132312/25.879513	331.6	63.5	5	235	5	-56.9	70.2	This study
HS41	46.135360/25.875348	352.3	64.0	6	148	5.5	-65.8	84.6	This study
HN15	46.120767/25.903083	33.3	63.9	5	147	6.3	105.1	66.9	[3]
HS37	46.121039/25.946081	59.5	64.0	5	199	5.4	94.1	49.6	This study
H7	46.113009/25.961221	18.4	73.5	9	804	1.5	58.9	72.8	[3]
Area mean direction and VGP									
Mean		1.0	66.6	44	40	3.4	26.0	85.3	This study

4. PALEOSECULAR VARIATION

The directional data, presented in Table 1 and Fig. 4, have a positive reversal test classification C according to [13]. The results from Table 1 fulfil the criteria of [1, 14] for paleosecular variation studies: number of samples per site minimum 5, precision parameter *k* larger than 50, confidence angle α_{95} less than 10°.

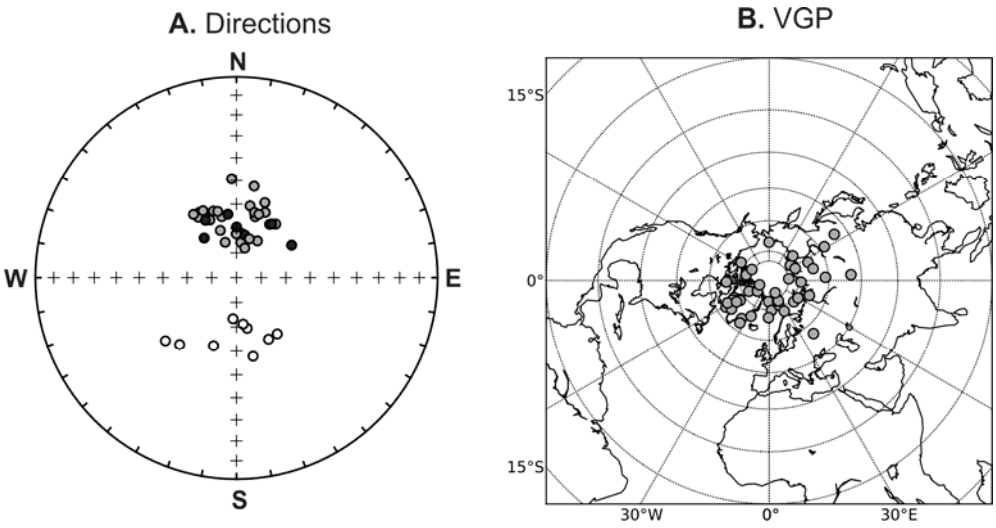

Fig. 4 – A. Site mean directions: full circles = normal polarity (grey – Perşani; black – Ciomadul); open circles = reversed polarity Perşani; B. Distribution of virtual geomagnetic poles (full circles). Reversed polarity VGPs were represented by their antipodes in the northern hemisphere.

The paleosecular variation of the geomagnetic field was expressed as the angular dispersion of VGPs [1, 14]. All VGPs have colatitudes less than 45°, so the angular dispersion was calculated using all the data from Table 1. We considered all data to be equally valid without trying to put neighboring flows into directional groups [15, 16]. The results are presented in Table 2. It must be note that the dispersion is similar with the one obtained by [4] using a smaller data set (26 sites).

Based on the data from the lava flows from the South Harghita [3], we have selected a group of 33 sites, which have the age between 2.8 Ma and 1.5 Ma (Pilişca and Cucu volcanic structures). The dispersion of VGPs was calculated without any arbitrary co-latitude cuff, because there is only one site which have a co-latitude large than 45°. The result is presented in Table 2. For comparison we have also presented the old results from [4].

Table 2

SB: the between-site VGP dispersion, along with 95% confidence limits (S_B^{lo}, S_B^{hi}); N is number of sites. References (Ref) for the data according to [4] and this study

Age (Ma)	Polarity	N	S_B (°)	S_B^{lo} (°)	S_B^{hi} (°)	Ref.
0.4-1.1	All combined	44	20.3	17.7	22.9	This study
0.6-1.1	All combined	26	19.6	16.7	22.3	[4]
1.5 – 2.8	All combined	33	26.0	21.5	29.6	This study
1.5-4.3	All combined	53	23.1	20.4	25.9	[4]

The dispersion of VGPs from this study is plotted in Fig. 5. In the same figure we presented the dispersion of VGPs according to the regional compilations for the Time Averaged geomagnetic Field Initiative (TAFI) studies and global compilation in the latitudinal band 42 °N–55 °N presented by [1]. The dispersion of VGPs observed in our 1.1–0.4 Ma data set is higher than that for the global compilation at 44.8°N latitude during Brunhes Chron (0–0.78 Ma), but it is in better agreement, at 95% confidence level, with dispersions obtained from the TAFI studies at the latitude of 43°N and the expected dispersion from geomagnetic field model TK03 [17]. Our analysis show that the high dispersion observed between 4.3–1.5 Ma by [3] is mainly produced in the time interval 2.8–1.5 Ma. The Matuyama data set (0.78–2.5 Ma) presented by [1] shows several estimates of SB around 53°N latitude that are higher than during the Brunhes chron (Fig. 5). The results from the Perşani and South Harghita Mountains might imply an increase of VGP dispersion during Matuyama chron starting around 45°N, but more data are necessary to confirm if this is a global characteristic of the geomagnetic field.

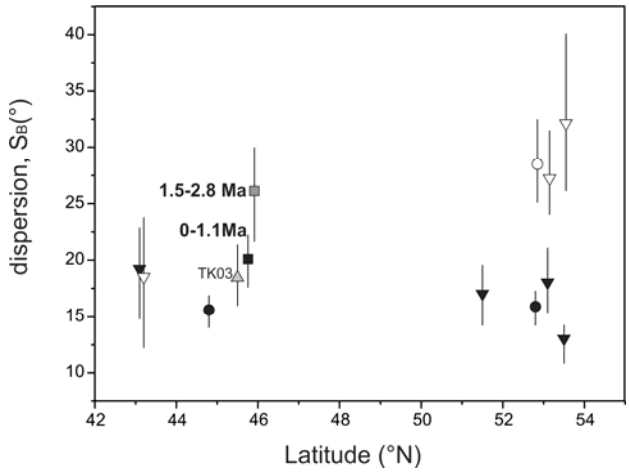

Fig. 5 – Dispersion of VGPs from this study (squares). Data from the Brunhes and the Matuyama chrons [1] are represented with black symbols and white symbols, respectively (inverted triangles = the TAFI studies; circles = the global compilation). Triangle marks the dispersion calculated from the TK03 model.

5. CONCLUSIONS

We have studied 4 new sites in the Ciomadu volcanic structure and 13 new sites in the basalts from the Perşani Mountains. The primary remanent magnetizations were successfully isolated from all these sites after demagnetizations. Based on these new data and previous results we have calculated the paleosecular variation of the geomagnetic field expressed as the dispersion of VGPs for two time interval 1.1–0.4 Ma and 2.8–1.5 Ma. Our new analysis shows that here is a significant increase of the dispersion of VGPs after 1 Ma around the latitude of 45°N. The results are similar with the global analysis [1] which shows a similar trend during the Matuyama chron with respect to the Brunhes chron.

Acknowledgements. This work was supported by a grant of the Ministry of National Education, CNCS – UEFISCDI, project number PN-II-ID-PCE-2012-4-0177. D.D. was supported by the project POSDRU/159/1.5/S/133391.

REFERENCES

1. C. L. Johnson, C. G. Constable, L.Tauxe, R. Barendregt, L. L.Brown, R. S. Coe, P. Layer, V. Mejia, N. D. Opdyke, B. S. Singer, H. Staudigel, D. B. Stone, Geochemistry, Geophysics, Geosystems **9**, Q04032 (2008).
2. C. Tanty, J. Carlut, J-P. Valet, A. Germa, Geophysical Journal International **200**, 917–934 (2015).
3. C.G. Panaiotu, M. Visan, A. Tugui, I. Seghedi, A. G. Panaiotu, Geophysical Journal International **189**, 369–382 (2012).
4. C. G. Panaiotu, B.R Jicha, B.S. Singer, A. Ţugui, I. Seghedi, A.G Panaiotu, C. Necula, Physics of the Earth and Planetary Interior **221**, 1–14 (2013).
5. A. Szakács, I. Seghedi, Z. Pécskay, V. Mirea, Bull Volcanol, **77**, *12* (2015); DOI 10.1007/s00445-014-0894-7.
6. M. Chadima, F. Hrouda, Travaux Géophysiques **XXVII**, 20–21 (2006).
7. L. Tauxe, *PmagPy, software package*; http://magician.ucsd.edu/Software/PmagPy/index.html
8. F. Hrouda, M. Chlupáčová, S. Mrázová, Physics of The Earth and Planetary Interiors **154**, 323–336 (2006).
9. M.E. Evans, F. Heller, *Environmental Magnetism: Principles and Applications of Environmagnetics*, Academic Press Elsevier Science, Amsterdam, 2003.
10. A. Ţugui, C. Necula, C. Panaiotu, Romanian Reports in Physics **61**, *3*, 730–739 (2009).
11. C. Panaiotu, C. Necula, T. Merezeanu, A. Panaiotu, C. Corban, Romanian Reports in Physics **63**, *2*, 526–534 (2011).
12. R. A Fisher, Proc. R. Soc. London, Ser. A **217**, 295–305 (1953).
13. P. L. McFadden, M. W. McElhinny, Geophys. J. Int. **103**, 725–729 (1990).
14. N. D. Opdyke, D. V. Kent, K. Huang, D. A. Foster, J. P. Patel, Geochem. Geophys. Geosyst. 11, Q05005 (2010); DOI: 10.1029/2009GC002863.
15. N. Suttie, A. Biggin, R. Holme, Geophys. J. Int., **200**, 1046–1051(2015)
16. C.G.A. Harrison, Geochem. Geophys. Geosyst. **10**, Q02012 (2009); DOI: 10.1029/ 2008GC002298.
17. L. Tauxe, D. Kent, *A simplified statistical model for the geomagnetic field and the detection of shallow bias in paleomagnetic inclinations: Was the ancient magnetic field dipolar?*, in: J.E.T. Channell, D.V. Kent, W. Lowrie, J.G. Meert (Editors), *Timescales of the Internal Geomagnetic Field*, Geophys. Monogr. Ser., AGU, Washington, D. C., 2004, pp. 101–115.